

Daratumumab Immunopolymerosome-Enabled Safe and CD38-Targeted Chemotherapy and Depletion of Multiple Myeloma

Na Yu, Yifan Zhang, Jiaying Li, Wenxing Gu, Shujing Yue, Bin Li, Fenghua Meng, Huanli Sun,* Rainer Haag, Jiandong Yuan, and Zhiyuan Zhong*

Multiple myeloma (MM) is a second ranking hematological malignancy. Despite the fast advancement of new treatments such as bortezomib and daratumumab, MM patients remain incurable and tend to eventually become relapsed and drug-resistant. Development of novel therapies capable of depleting MM cells is strongly needed. Here, daratumumab immunopolymerosomes carrying vincristine sulfate (Dar-IPs-VCR) are reported for safe and high-efficacy CD38-targeted chemotherapy and depletion of orthotopic MM in vivo. Dar-IPs-VCR made by postmodification via strain-promoted click reaction holds tailored antibody density (2.2, 4.4 to 8.7 Dar per IPs), superb stability, small size (43–49 nm), efficacious VCR loading, and glutathione-responsive VCR release. Dar_{4.4}-IPs-VCR induces exceptional anti-MM activity with an IC₅₀ of 76×10^{-12} M to CD38-positive LP-1 MM cells, 12- and 20-fold enhancement over nontargeted Ps-VCR and free VCR controls, respectively. Intriguingly, mice bearing orthotopic LP-1-Luc MM following four cycles of i.v. administration of Dar_{4.4}-IPs-VCR at 0.25 mg VCR equiv. kg⁻¹ reveal complete depletion of LP-1-Luc cells, superior survival rate to all controls, and no body weight loss. The bone and histological analyses indicate bare bone and organ damage. Dar-IPs-VCR appears as a safe and targeted treatment for CD38-overexpressed hematological malignancies.


liposomes and polymeric nanosystems has been a major strategy and obtained booming development.^[2] Amidst them, antibody and antibody fragment decorated immuno-nanomedicines have gained particular attention due to their high specificity and affinity, as evidenced by marketed antibody–drug conjugates^[3] and undergoing clinical trials of several immunoliposomes (e.g., MCC-465, MM-302, C225-ILs-DOX, and MM-310).^[4] The immuno-nanomedicines based on liposomes and polymeric nanoparticles (e.g., poly(lactic-co-glycolic acid)) though have shown enhanced tumor cell uptake and good safety brought about only moderate therapeutic benefits,^[5] partly due to their large size, insufficient stability, suboptimal ligand density, and premature drug leakage. The lack of robust and small-sized nanosystem that allows stable drug loading and facile and controllable antibody conjugation is a major hurdle for clinical translation of targeted immuno-nanomedicines.

The development of actively targeted nanotherapeutics to realize specific homing and augmented retention in the tumor site as well as boosted internalization by tumor cells is a primary goal of nanomedicine for revolutionizing cancer treatment.^[1] Installing affinity ligands such as peptides, small molecules, antibodies and their fragments onto the surface of

Multiple myeloma (MM), the second most common hematological malignancy, remains incurable and tends to eventually become relapsed and drug-resistant.^[6] Daratumumab (Dar), the first-in-class CD38-specific IgG1κ monoclonal antibody, has recently emerged as a new treatment regime for relapsed/refractory and newly diagnosed MM patients due to the relatively specific overexpression of CD38

N. Yu, Y. F. Zhang, W. X. Gu, S. J. Yue, Prof. F. H. Meng, Dr. H. L. Sun, Prof. Z. Y. Zhong
 Biomedical Polymers Laboratory
 College of Chemistry
 Chemical Engineering and
 Materials Science
 State Key Laboratory of Radiation Medicine and Protection
 Soochow University
 Suzhou 215123, P. R. China
 E-mail: sunhuanli@suda.edu.cn; zyzhong@suda.edu.cn

J. Y. Li, Prof. B. Li
 Department of Orthopaedic Surgery
 Orthopaedic Institute
 The First Affiliated Hospital
 Soochow University
 Suzhou 215007, P. R. China
 Prof. R. Haag
 Department of Biology
 Chemistry and Pharmacy
 Institute for Chemistry and Biochemistry
 Freie Universität Berlin
 14195 Berlin, Germany
 Dr. J. D. Yuan
 BrightGene Bio-Medical Technology Co, Ltd
 Suzhou 215123, P. R. China

 The ORCID identification number(s) for the author(s) of this article can be found under <https://doi.org/10.1002/adma.202007787>.

DOI: 10.1002/adma.202007787

on the surface of MM cells.^[7] Either as a monotherapy^[8] or in combination with other small molecular agents (e.g., lenalidomide, bortezomib, dexamethasone, etc.),^[9] Dar has exhibited promising anti-MM activity with significant clinical responses in both frontline and relapsed/refractory settings. In spite of the durable responses, Dar-treated patients eventually suffer relapse and severe systemic toxicity as a result of the development of drug resistance and high dose administration.^[10]

Herein, we report on a facile strategy to construct robust daratumumab immunopolymersomes that mediate safe and CD38-targeted delivery of vincristine sulfate (Dar-IPs-VCR) leading to depletion of orthotopic MM (Figure 1a–c). Dar-IPs-VCR is fabricated with efficacious VCR loading, superb stability, small size, and tailored antibody density by postmodification via strain-promoted click reaction. VCR is a water-soluble and powerful drug for MM and leukemia treatment in the clinics.^[11] Intriguingly, Dar_{4.4}-IPs-VCR induced 12- and 20-fold better anti-MM activity to CD38-positive LP-1 MM cells than nontargeted Ps-VCR and free VCR controls, respectively, and mice bearing orthotopic LP-1-Luc MM following four cycles of i.v. administration of Dar_{4.4}-IPs-VCR at a low dose of 0.25 mg VCR equiv. kg^{−1} revealed complete depletion of LP-1-Luc cells, superior survival rate to all controls, and no body weight loss. Dar-IPs-VCR appears as a safe and targeted treatment for CD38-overexpressed hematological malignancies.

Dar-IPs-VCR was engineered by strain promoted click reaction of dibenzocyclooctyne-functionalized Dar (Dar-DBCO) with azide-functionalized polymersomal VCR (N₃-Ps-VCR), which was constructed from coassembly of azide-functionalized poly(ethylene glycol)-*b*-poly(trimethylene carbonate-co-dithiolane trimethylene carbonate) (N₃-PEG-P(TMC-DTC)) and PEG-P(TMC-DTC)-KD₅ (weight ratio: 2/98) with simultaneous VCR loading through electrostatic interactions. N₃-PEG-P(TMC-DTC) with a molecular weight of 7.9–(14.9–2.1) kg mol^{−1} and M_w/M_n of 1.1 was synthesized by ring-opening copolymerization of TMC and DTC using N₃-PEG-OH as a macroinitiator (Figures S1a and S2a, Supporting Information). Through activating the terminal hydroxyl group of PEG-P(TMC-DTC) (5.0–(15.0–2.0) kg mol^{−1}, M_w/M_n = 1.1) and subsequent reaction with KD₅ peptide as in our previous report,^[12] PEG-P(TMC-DTC)-KD₅ was obtained with a KD₅ conjugation degree of ≈100%, as determined by ¹H NMR and high-performance liquid chromatography (Figures S1b and S2b,c, Supporting Information). By simply injecting the polymer solution in dimethyl sulfoxide to *N*-(2-hydroxyethyl) piperazine-*N'*-(2-ethanesulfonic acid) buffer, N₃-Ps was prepared with an aggregation number of ≈521 and 9.2 N₃ groups each on average (Figure S3, Supporting Information). N₃-Ps-VCR displayed a size of 36 nm, a low polydispersity (PDI: 0.11) and high VCR loading efficiency of 97.2% at a theoretical drug loading content (DLC) of 4.8 wt%. The size of N₃-Ps-VCR was much smaller than the reported VCR nanoformulations including clinically used liposomal VCR (Marqibo).^[13] In addition, unlike other VCR nanosystems with insufficient stability, its concentrated formulation (42 nm, PDI: 0.07) at a Ps concentration of 18.6 mg mL^{−1} possessed superb stability during 6 months storage in the fridge, wherein, size was maintained around 40 nm with PDI < 0.17 and VCR retention rate was over 99.4% (Figure 1d). To acquire Dar-IPs-VCR, Dar-DBCO_{1.5} with an average of 1.5 DBCO per Dar was

prepared firstly via reaction of Dar with threefold molar excess of DBCO-PEG₄-*N*-hydroxysuccinimidyl ester (Figure S4a, Supporting Information) and then reacted with N₃-Ps-VCR. By adjusting the molar ratios of Dar-DBCO to N₃ from 0.25:1, 0.5:1 to 1:1, Dar-IPs-VCR with 2.2, 4.4, and 8.7 of Dar per polymerosome (denoted as Dar_{*x*}-IPs-VCR, *x* is Dar density), respectively, were obtained at conjugation efficiencies of more than 94% (Table S1, Supporting Information). The size of Dar-IPs-VCR increased slightly from 43 to 49 nm with increasing Dar density while the size distribution was all narrow (PDI: 0.14–0.21) (Figure 1e and Table S1, Supporting Information). Importantly, little VCR leaked out during the postmodification and work-up procedure. Moreover, Dar conjugated on the surface of polymersomes maintained a comparable secondary structure to that of native Dar, as shown by circular dichroism (CD) spectra (Figure S4b, Supporting Information). Similar to other disulfide-crosslinked nanosystems,^[14] Dar-IPs-VCR was stable against either 50-fold dilution or incubation in 10% fetal bovine serum for 24 h (Figure S5, Supporting Information) showing diminished VCR leakage under physiological condition, while released 85% of VCR in 12 h upon treatment with 10 × 10^{−3} M GSH (Figure 1f). This good balance between stability and intracellular drug release of Dar-IPs-VCR is superior to that of the reported immuno-nanosystems, which showed drug leakage during storage while slow and fractional drug release inside cells.^[15]

It is reported that CD38 is uniformly overexpressed on MM cells and represents a promising target for MM treatment, as demonstrated by the successful clinical translation of several anti-CD38 antibodies.^[16] Herein, CD38 expression levels of LP-1 and MM.1S MM cells as well as MV4-11 acute myeloid leukemia (AML) cells were examined via flow cytometry using phycoerythrin (PE)-labeled antihuman-CD38 antibody. The results revealed that CD38 was highly expressed on LP-1 cells and moderately expressed on MM.1S cells with a level of around 488- and 17-fold higher than that on MV4-11 cells, respectively (Figure 2a and Figure S6a, Supporting Information). LP-1 cells were hereafter utilized to investigate the CD38-targeted cellular uptake, anti-MM efficacy and apoptotic ability of Dar-IPs-VCR, and MV4-11 cells were used as a CD38-negative control. In order to visualize the cellular uptake, Cy5 labeled Dar-IPs (Dar-IPs-Cy5) with different Dar densities and Ps-Cy5 were engineered and employed for flow cytometry and confocal laser scanning microscopy (CLSM) studies. Compared to nontargeted Ps-Cy5 control, Dar-IPs-Cy5 with 2.2, 4.4, and 8.7 Dar on each Ps all displayed markedly higher cellular internalization in LP-1 cells after 4 h incubation, wherein, Dar_{4.4}-IPs-Cy5 possessed the best targetability showing 6.4-fold higher cellular uptake (Figure 2b), outperforming A6 peptide and hyaluronic acid decorated polymersomes.^[17] The internalization of Dar_{4.4}-IPs-Cy5 was markedly repressed by clathrin/dynamin endocytic inhibitors chlorpromazine and dynasore (Figure S7, Supporting Information), in line with a receptor-mediated endocytosis mechanism. The endocytosis was also partially inhibited by amiloride hydrochloride, signifying that macropinocytosis plays a role as well. CLSM images displayed strong Cy5 fluorescence in the intracellular perinuclear region of LP-1 cells after 4 h incubation with Dar_{4.4}-IPs-Cy5, while much weaker Cy5 signal was observed in Ps-Cy5 treated cells (Figure S8, Supporting

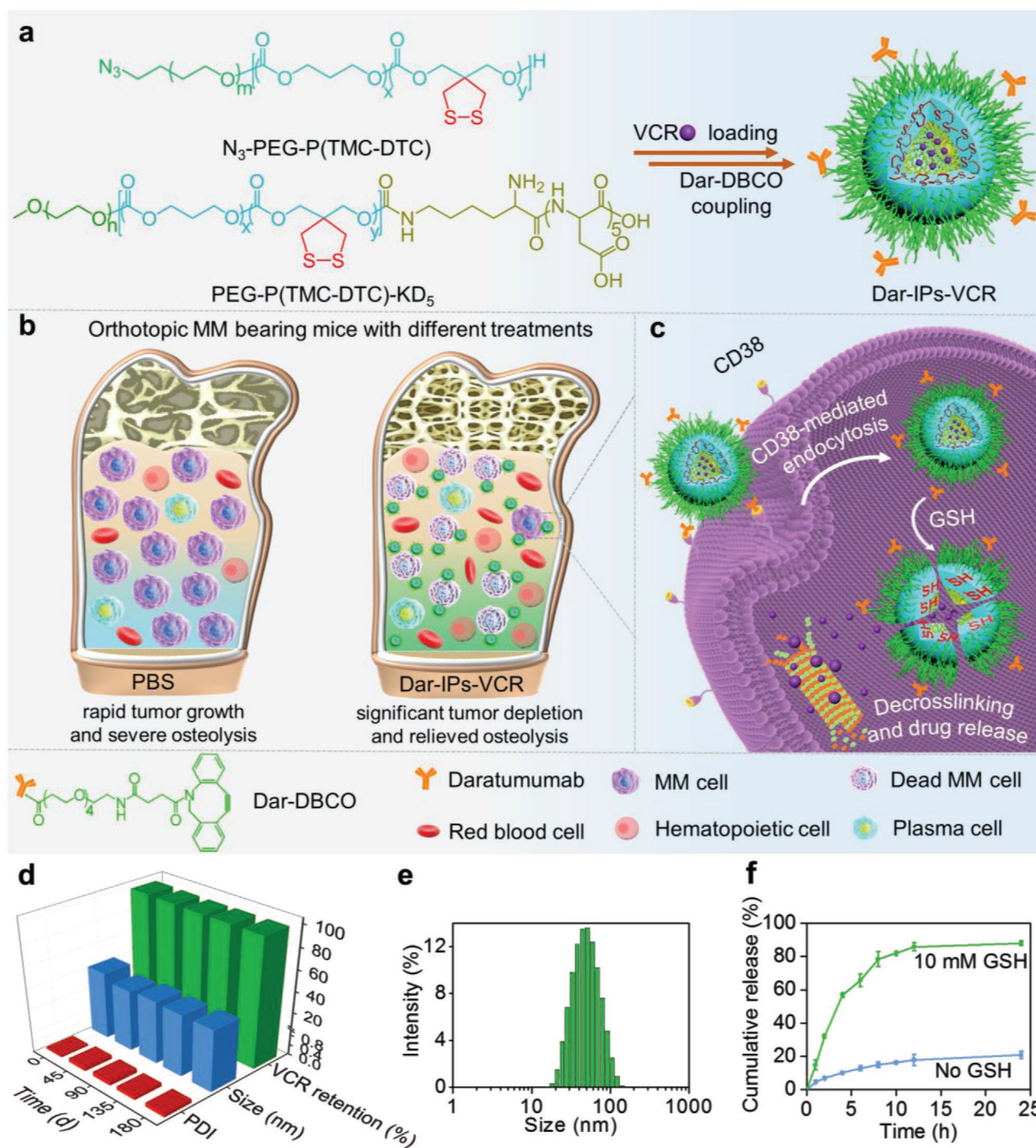
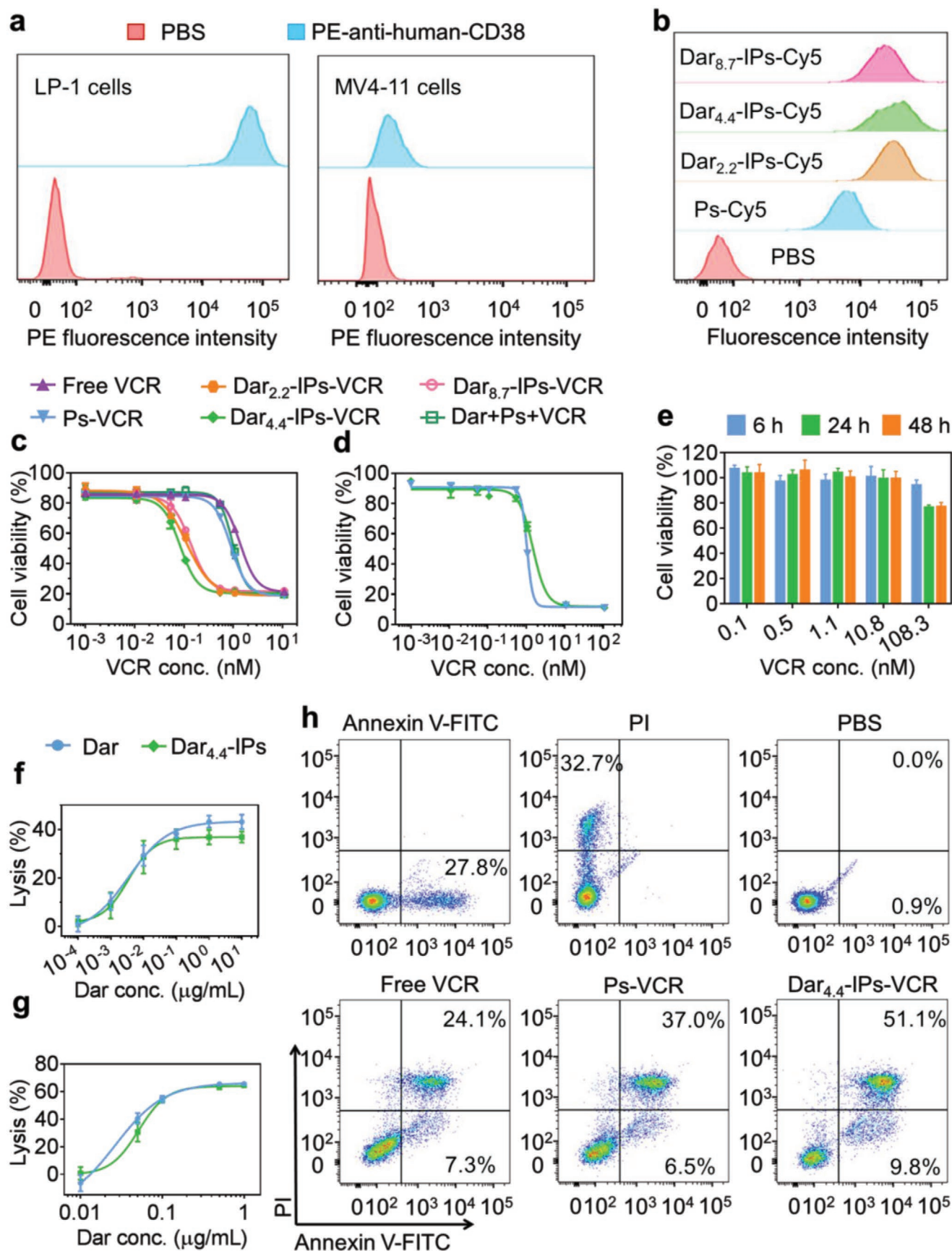


Figure 1. Illustration of daratumumab immunopolymerosomes carrying vincristine sulfate (Dar-IPs-VCR) for CD38-specific targeting and potent depletion of orthotopic LP-1-Luc MM in vivo. a) Dar-IPs-VCR is constructed via coassembly of N_3 -PEG-P(TMC-DTC) and PEG-P(TMC-DTC)-KD₅ block copolymers with simultaneous VCR loading through electrostatic interactions, followed by strain-promoted click reaction with Dar-DBCO. b) Dar-IPs-VCR significantly suppresses MM growth and relieves osteolysis as a result of CD38-specific binding to MM cells in the bone marrow with sequentially CD38-mediated cellular uptake and glutathione (GSH)-triggered VCR release for inhibiting microtubule formation and causing cell apoptosis (c). d) Long-term storage stability of N_3 -Ps-VCR at 4 °C. e) Size distribution of Dar-IPs-VCR determined via dynamic light scattering. f) In vitro VCR release profiles of Dar-IPs-VCR in the presence or absence of 10×10^{-3} M GSH ($n = 3$).

Information), further indicating the CD38-targeting capability and significantly enhanced cellular uptake of Dar-IPs-Cy5 in LP-1 cells. Consistently, Dar-IPs-VCR bearing different Dar

densities were all potent to CD38-positive LP-1 cells and Dar_{4.4}-IPs-VCR had the lowest half-maximal inhibitory concentration (IC₅₀) of 76×10^{-12} M (Figure 2c), which was two to five orders



of magnitude lower than CD44-targeted granzyme B, bortezomib, and epirubicin (EPI) nanomedicines in LP-1 cells.^[17,18] Moreover, Dar_{4,4}-IPs-VCR was 20-, 14- and 12-fold more potent compared to free VCR (1.5×10^{-9} M), Dar+Ps+VCR mixture (VCR: 1.1×10^{-9} M) and Ps-VCR (0.9×10^{-9} M), respectively. In MM.1S cells with moderate CD38 expression, Dar_{4,4}-IPs-VCR induced 2.8-fold higher cytotoxicity (IC_{50} : 0.42×10^{-9} M) than Ps-VCR (1.17×10^{-9} M), confirming the CD38-mediated endocytosis of Dar_{4,4}-IPs-VCR in CD38-overexpressed MM cells (Figure S6b, Supporting Information). In contrast, for CD38-negative MV4-11 cells, Dar_{4,4}-IPs-VCR induced similar toxicity to Ps-VCR with an IC_{50} of about 1.5×10^{-9} M, which was around 20-fold higher than Dar_{4,4}-IPs-VCR in LP-1 cells (Figure 2d). More interestingly, Dar_{4,4}-IPs-VCR were nearly nontoxic to peripheral blood mononuclear cells (PBMCs) isolated from a normal donor and L929 normal cells even at a VCR concentration as high as 108.3×10^{-9} M (Figure 2e and Figure S9, Supporting Information). It is obvious that Dar_{4,4}-IPs-VCR can selectively target and induce potent toxicity to CD38-positive MM cells, while sparing normal cells. Moreover, blank Dar_{4,4}-IPs and Ps as well as native Dar were nontoxic to LP-1 cells at a Ps concentration of $30 \mu\text{g mL}^{-1}$ and Dar concentration of 60×10^{-9} M (Figure S10, Supporting Information). However, in the presence of PBMCs or human serum, Dar_{4,4}-IPs, similar as native Dar, caused dose-dependent lysis of LP-1 cells (Figure 2f,g), indicating Dar decorated on the polymersome surface maintained its strong ability to mediate antibody-dependent cell-mediated cytotoxicity (ADCC) and complement-dependent cytotoxicity (CDC). Of note, the effective Dar concentration for ADCC and CDC was above 0.1 and 10 ng mL⁻¹, respectively, which were higher than Dar in Dar_{4,4}-IPs-VCR of IC_{50} value (0.08 ng Dar equiv. mL⁻¹). Apoptosis assays further showed that Dar_{4,4}-IPs-VCR induced much higher cell apoptosis (60.8%) at a VCR concentration of 0.5×10^{-9} M than Ps-VCR (43.4% and 31.4%) (Figure 2h). Interestingly, for human T cells, Dar_{4,4}-IPs-VCR treatment at VCR concentrations of 0.01 – 0.5×10^{-9} M exhibited comparable apoptosis profile to phosphate buffered saline (PBS) (Figure S11, Supporting Information), supporting that Dar_{4,4}-IPs-VCR has a low toxicity. It is known that VCR suppresses cancer cell proliferation via inhibiting microtubule formation in mitotic spindle and therefore causes cell cycle arrest in the metaphase.^[19] As expected, Dar_{4,4}-IPs-VCR more efficiently reduced the expression of β -tubulin in LP-1 cells than Ps-VCR and free VCR, as shown by western blot results (Figure S12, Supporting Information). These results corroborate that Dar_{4,4}-IPs-VCR can selectively target CD38-positive MM cells with rapid cellular internalization and intracellular VCR release, leading to reduced tubulin expression, increased cell apoptosis, and potent cell growth inhibition. In a similar way, we have also prepared doxorubicin hydrochloride-loaded daratumumab immunopolymersomes (Dar_{5,5}-IPs-DOX) with a size of 42 nm and DLC of 4.0 wt%.

The results confirmed that Dar significantly enhanced uptake and cytotoxicity of Ps-DOX in LP-1 cells (IC_{50} : 0.16×10^{-6} M for Dar_{5,5}-IPs-DOX vs 0.61×10^{-6} M for Ps-DOX) (Figure S13, Supporting Information).

In vivo acute toxicity studies showed that Dar_{4,4}-IPs-VCR can reduce side effects and widen the therapeutic window of VCR, wherein, mice displayed survival rates of 100% and 80% at VCR dosage of 2.0 and 3.0 mg kg⁻¹, respectively (Figure S14, Supporting Information). However, when dosed with free VCR, all mice died at 2.0 mg kg⁻¹ and suffered significant abnormalities in blood counts even at 1.0 mg kg⁻¹ (Figures S14 and S15, Supporting Information). To evaluate the in vivo anti-MM performance of Dar_{4,4}-IPs-VCR, orthotopic LP-1-Luc MM model was established via tail vein injection of LP-1-Luc cells in cyclophosphamide (CTX) pretreated NOD/SCID (nonobese diabetic/severe combined immunodeficiency) mice (Figure 3a). On day 35 after LP-1-Luc inoculation, mice developed classic symptoms of hind limb weakness and paralysis, as that for MM patients.^[20] Ex vivo bioluminescence images further displayed strong Luc signals in the hind legs and skull of mice (Figure S16, Supporting Information), supporting the successful construction of an orthotopic LP-1-Luc MM model. In vivo fluorescence image of orthotopic LP-1-Luc MM bearing mice at 8 h after i.v. injection of Dar_{4,4}-IPs-Cy5 showed bright Cy5 signal in the legs and head where LP-1-Luc cells mainly infiltrated, and the Cy5 fluorescence was remarkably stronger than Ps-Cy5 treated mice (Figure 3b). Anti-MM studies were initiated on day 10 post-LP-1-Luc inoculation when the luminescence intensity reached $\approx 1.2 \times 10^6$ p s⁻¹ cm⁻² sr⁻¹ and were continuously monitored via bioluminescence imaging (Figure 3a). Following four cycles of i.v. administration of Dar_{4,4}-IPs-VCR at 0.25 mg VCR equiv. kg⁻¹, mice bearing orthotopic LP-1-Luc MM revealed complete depletion of LP-1-Luc cells over the whole imaging period, showing comparable luminescence level to the background signal of healthy mice (Figure 3c,d). However, the proliferation of LP-1-Luc cells in free VCR, Ps-VCR and Dar+Ps+VCR mixture treated groups was renewed immediately after the last administration inducing rapid MM progression (Figures 3c,d and S17, Supporting Information). PBS treated mice displayed dramatic luminescence increase by ≈ 4800 -fold from day 10 to 39 and experienced noticeable symptoms and even death. Notably, mice following treatment with native Dar and Dar_{4,4}-IPs at a Dar dosage of 0.59 mg kg⁻¹ exhibited a similar luminescence increase profile as PBS group (Figure S17, Supporting Information). Even at a high Dar dosage of 14.56 mg kg⁻¹, which is 50-fold higher than that in Dar_{4,4}-IPs-VCR group, native Dar and Dar_{4,4}-IPs induced insignificant growth inhibition of MM compared to PBS (Figure S18, Supporting Information). These results corroborated that Dar_{4,4}-IPs-VCR was competent in targeted delivery of VCR to MM cells and eradicating MM. The minimal amount of Dar used in Dar_{4,4}-IPs-VCR does not cause ADCC or CDC. Moreover, according to the previous

Figure 2. a) CD38 expression on the surface of LP-1 and MV4-11 cells, as determined by flow cytometry. b) Fluorescence intensity of LP-1 cells after 4 h incubation with Dar-IPs-Cy5 bearing different Dar densities quantified via flow cytometry. c,d) In vitro antitumor effect of Dar-IPs-VCR with different Dar densities, free VCR and Dar+Ps+VCR mixture against CD38-positive LP-1 cells (c) and CD38-negative MV4-11 cells (d) following 48 h incubation evaluated by cell counting kit-8 assays ($n = 4$). e) In vitro cytotoxicity of Dar_{4,4}-IPs-VCR in PBMCs with different incubation time (6, 24, and 48 h). f,g) Dar_{4,4}-IPs and native Dar induced ADCC (f) and CDC (g) against LP-1 cells. h) Apoptosis of LP-1 cells after 48 h treatment with Dar_{4,4}-IPs-VCR, Ps-VCR, or free VCR at a VCR concentration of 0.5×10^{-9} M.

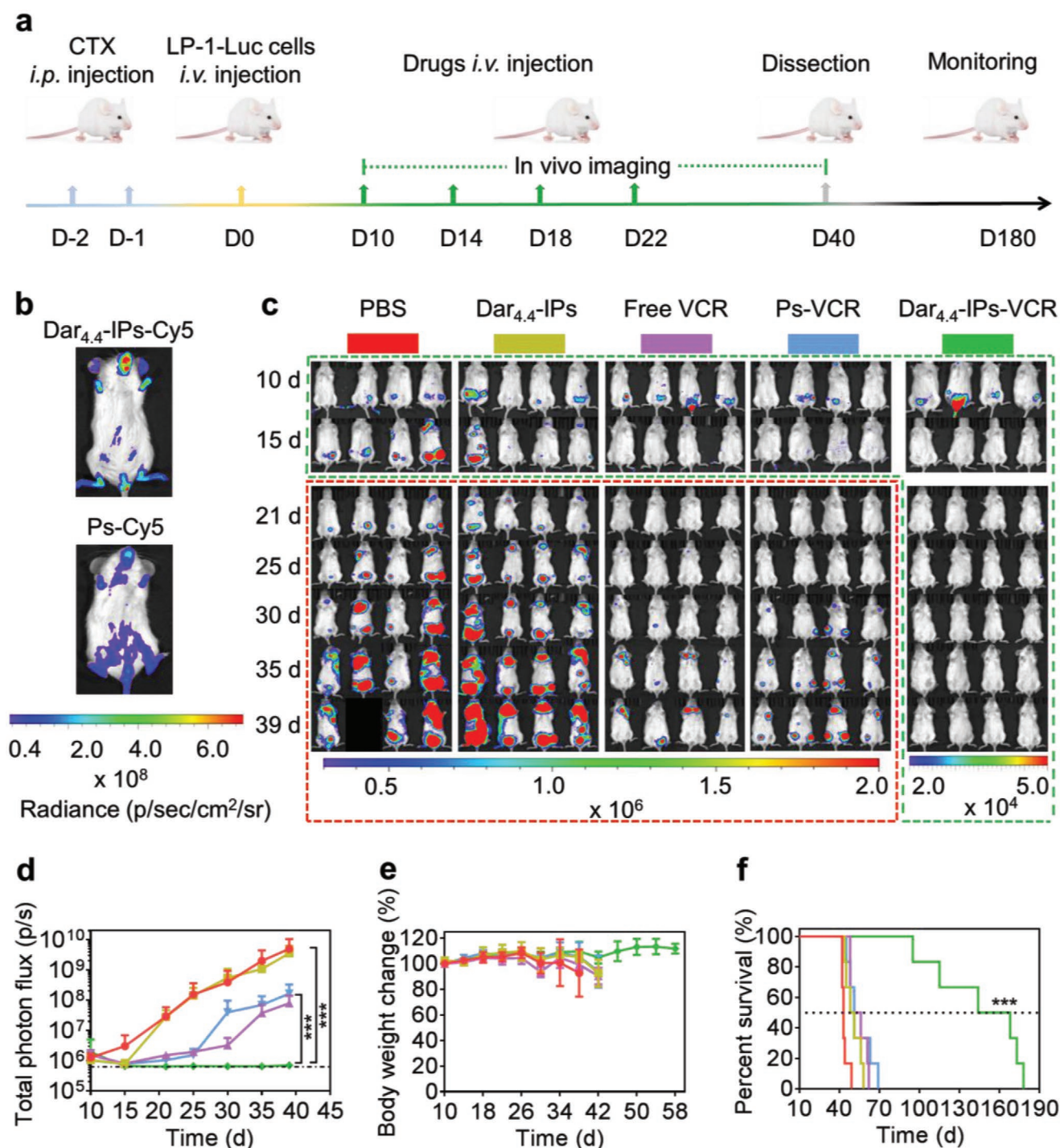


Figure 3. In vivo anti-MM study of Dar_{4,4}-IPs-VCR in orthotopic LP-1-Luc MM bearing mice, Ps-VCR, free VCR, Dar_{4,4}-IPs, and PBS were employed as controls. a) Schematic showing the establishment, treatment, and monitoring schedule of orthotopic LP-1-Luc MM model. b) Cy5-fluorescence imaging of mice at 8 h post *i.v.* injection of Dar_{4,4}-IPs-Cy5 and Ps-Cy5. c) Bioluminescence imaging of mice following different treatments from day 10 to day 39 (n = 4). d) Quantitative luminescence intensities of mice in (c), dashed line represents background luminescence signal of healthy mice. e) Body weight changes of mice within 58 d (n = 6). f) Kaplan–Meier survival curves of mice in different treatment groups (n = 6, Dar_{4,4}-IPs-VCR vs Ps-VCR, free VCR, Dar_{4,4}-IPs and PBS, *** P < 0.001).

report,^[17a] mice bearing orthotopic LP-1-Luc MM post-treatment with A6-Ps-EPI remain burdened by obvious MM with strong luminescence signals. Importantly, Dar_{4,4}-IPs-VCR and Ps-VCR

treated mice gained weight steadily during the administration period (Figure 3e), confirming their superior safety. Figure 3f shows that Dar_{4,4}-IPs-VCR significantly prolonged the survival

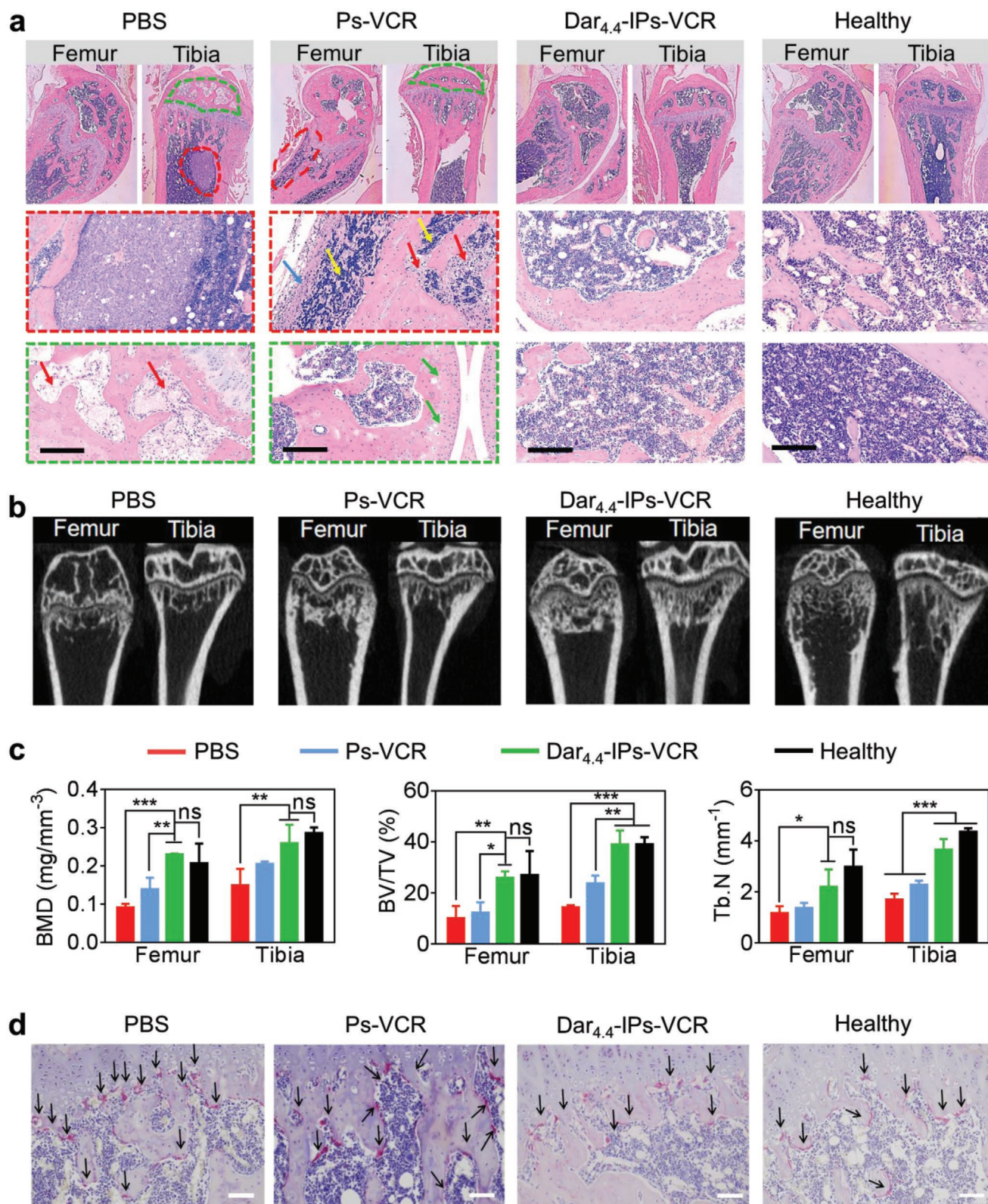


Figure 4. Analysis of femur and tibia of orthotopic MM bearing mice in different treatment groups. a) H&E staining images for histological analysis, red arrows indicate the reduction of hematopoietic cells; the blue arrow indicates osteonecrosis; the yellow arrows indicate oat cell hyperplasia; the green arrows indicate chondrocyte necrosis; scale bars: 200 μ m. b) Micro-CT images. c) Quantitative analysis of BMD, BV/TV, and Tb.N ($n = 4$), * $P < 0.05$, ** $P < 0.01$, *** $P < 0.001$. d) TRAP staining images for identifying osteoclasts; scale bars: 400 μ m.

of orthotopic LP-1-Luc MM bearing mice, displaying a median survival time of 156 d which was 3.0–3.6-fold longer than that of PBS (43 d), Dar_{4,4}-IPs (49.5 d), Ps-VCR (51 d) and free VCR (52 d) groups. The survival benefits from Dar_{4,4}-IPs-VCR treatment were exceptional compared with A6-Ps-VCR (median survival time of 80 d, Figure S19, Supporting Information) and previously reported alendronate,^[21] VLA-4-peptide (where VLA = very late antigen),^[22] and hyaluronic acid^[17b] decorated nanomedicines. Furthermore, two injections of Dar_{4,4}-IPs-VCR on day 10 and 18 at a VCR dosage of 0.5 mg kg⁻¹ also effectively depleted the LP-1-Luc cells, leading to a median survival time of 154 d (Figure S20, Supporting Information). Of note, anti-CD38 antibody decorated chitosan nanoparticles and poly(ethylene oxide)-*b*-poly(α -benzyl carboxylate- ϵ -caprolactone) nanoparticles incorporating bortezomib and STAT3 inhibitor, respectively, were reported with only slightly improved therapeutic index and survival benefits, likely due to their insufficient stability and uncontrollable drug release.^[23]

Histological analyses of hematoxylin and eosin (H&E) stained femur and tibia exhibited that Dar_{4,4}-IPs-VCR treated mice had similar hematopoietic tissue and bone histomorphology to healthy mice (Figure 4a). It was in stark contrast to PBS and Ps-VCR treated mice suffering a sharp reduction of hematopoietic cells and/or visible tumor infiltration in the bone marrow. It is well known that osteolysis is one of the most common clinical manifestations for MM patients.^[24] Micro-computer tomography (micro-CT) was hence utilized to evaluate the femur and tibia of mice following different treatments. The images showed that PBS treated mice suffered severe bony destruction and trabecular bone loss, which were, however, effectively relieved for Dar_{4,4}-IPs-VCR group, presenting a similar bone structure to that of healthy mice (Figure 4b). Ps-VCR, although alleviated the osteolysis, was much less effective compared to Dar_{4,4}-IPs-VCR. Quantitative analyses (Figure 4c and Figure S21, Supporting Information) further exhibited that unlike PBS and Ps-VCR groups, mice treated with Dar_{4,4}-IPs-VCR had comparable femoral and tibial indicators including bone mineral density (BMD), bone volume fraction (BV/TV), trabecular number (Tb.N), bone surface area, trabecular separation, and thickness to healthy mice. The underlying cause behind osteolysis is the disruption of the balance between osteoclasts and osteoblasts, wherein, increased osteoclasts induced bone resorption.^[25] Tartrate-resistant acid phosphatase (TRAP) staining, as one of the main strategy to identify osteoclasts,^[26] revealed that Dar_{4,4}-IPs-VCR treated group had less osteoclasts than PBS and Ps-VCR treated groups (Figure 4d). Furthermore, Dar_{4,4}-IPs-VCR treatment restored the blood routine and biochemical parameters to a similar level as healthy mice, efficaciously alleviating the symptoms of erythropenia, thrombocytopenia and elevated blood urea (Figure S22, Supporting Information), which are common for MM patients.^[6c,27] It is evident that Dar_{4,4}-IPs-VCR has superior anti-MM efficacy, thus inhibits MM-associated anemia and osteolysis. Of note, H&E staining showed no obvious pathological changes in the major organs for Dar_{4,4}-IPs-VCR group (Figure S23, Supporting Information), certifying that it has low side effects.

In conclusion, we have demonstrated that daratumumab immunopolymersomes enable safe and CD38-targeted delivery of vincristine sulfate (Dar-IPs-VCR), leading to extremely potent

and selective depletion of orthotopic MM in mice. Of note, these novel daratumumab immunopolymersomes not only boost the efficacy of chemotherapy but also mitigate drug-associated adverse effects and further widen therapeutic windows. To the best of our knowledge, this is a first report on highly robust and small-sized biodegradable nanosystems that facilitate controlled postmodification with monoclonal antibodies, which provides a unique and highly promising platform for targeted chemotherapy.

Supporting Information

Supporting Information is available from the Wiley Online Library or from the author.

Acknowledgements

N.Y. and Y.Z. contributed equally to this work. This work was supported by the National Natural Science Foundation of China (51633005, 52073196, and 51761135117), the Natural Science Foundation of Jiangsu Province (BK20160322), and the German Science Foundation (DFG). All animal experiments were approved by the Animal Care and Use Committee of Soochow University (P. R. China) and all protocols of animal studies conformed to the Guide for the Care and Use of Laboratory Animals. Blood of two healthy volunteers was drawn for isolating PBMCs for in vitro cell toxicity and ADCC studies, which was approved by the Ethical Committee of Institute of the First Affiliated Hospital of Soochow University, and the volunteers gave informed written consent. The authors thank Dr. Jingnan An and Dr. Tianhui Liu from the First Affiliated Hospital of Soochow University for providing MM and AML cells. The authors thank Dr. Fengtao You from Persongen Bio Therapeutics (Suzhou) Co., Ltd and Tingting Zhang from Cyrus Tang Medical Institute of Soochow University for providing T cells and kind help in apoptosis experiment of T cells.

Conflict of Interest

The authors declare no conflict of interest.

Data Availability Statement

Research data are not shared.

Keywords

CD38, multiple myeloma, nanomedicines, polymersomes, targeted chemotherapy

Received: November 16, 2020

Revised: May 27, 2021

Published online:

- [1] a) J. Shi, P. W. Kantoff, R. Wooster, O. C. Farokhzad, *Nat. Rev. Cancer* **2017**, 17, 20; b) D. Rosenblum, N. Joshi, W. Tao, J. M. Karp, D. Peer, *Nat. Commun.* **2018**, 9, 1410; c) H. Yuan, W. Jiang, C. A. von Roemeling, Y. Qie, X. Liu, Y. Chen, Y. Wang, R. E. Wharen, K. Yun, G. Bu, K. L. Knutson, B. Y. S. Kim, *Nat. Nanotechnol.* **2017**, 12, 763.

- [2] a) W. S. Kamoun, D. B. Kirpotin, Z. R. Huang, S. K. Tipparaju, C. O. Noble, M. E. Hayes, L. Luus, A. Koshkaryev, J. Kim, K. Olivier, T. Kornaga, S. Oyama, V. Askoxylakis, C. Pien, G. Kuesters, N. Dumont, A. A. Lugovskoy, S. A. Schihl, J. H. Wilton, M. L. Geddie, J. Suchy, S. Grabow, N. Kohli, C. P. Reynolds, R. Blaydes, Y. Zhou, A. J. Sawyer, J. D. Marks, D. C. Drummond, *Nat. Biomed. Eng.* **2019**, 3, 264; b) T. M. Allen, *Nat. Rev. Cancer* **2002**, 2, 750; c) A. David, *Adv. Drug Delivery Rev.* **2017**, 119, 120; d) P. Mi, H. Cabral, K. Kataoka, *Adv. Mater.* **2020**, 32, 29.
- [3] a) P. J. Carter, G. A. Lazar, *Nat. Rev. Drug Discovery* **2018**, 17, 197; b) C. H. Chau, P. S. Steeg, W. D. Figg, *Lancet* **2019**, 394, 793; c) A. Beck, L. Goetsch, C. Dumontet, N. Corvaia, *Nat. Rev. Drug Discovery* **2017**, 16, 315.
- [4] a) J. Di, F. Xie, Y. Xu, *Adv. Drug Delivery Rev.* **2020**, 154–155, 151; b) H. He, L. Liu, E. E. Morin, M. Liu, A. Schwendeman, *Acc. Chem. Res.* **2019**, 52, 2445.
- [5] a) C. Mamot, R. Ritschard, A. Wicki, G. Stehle, T. Dieterle, L. Bubendorf, C. Hilker, S. Deuster, R. Herrmann, C. Rochlitz, *Lancet Oncol.* **2012**, 13, 1234; b) P. Munster, I. E. Krop, P. LoRusso, C. Ma, B. A. Siegel, A. F. Shields, I. Molnar, T. J. Wickham, J. Reynolds, K. Campbell, B. S. Hendriks, B. S. Adiwijaya, E. Geretti, V. Moyo, K. D. Miller, *Br. J. Cancer* **2018**, 119, 1086; c) M. Merino, S. Zalba, M. J. Garrido, *J. Controlled Release* **2018**, 275, 162; d) D. M. Valcourt, M. N. Dang, M. A. Scully, E. S. Day, *ACS Nano* **2020**, 14, 3378.
- [6] a) S. K. Kumar, S. V. Rajkumar, *Nat. Rev. Clin. Oncol.* **2018**, 15, 409; b) A. J. Cowan, C. Allen, A. Barac, H. Basaleem, I. Bensenor, M. P. Curado, K. Foreman, R. Gupta, J. Harvey, H. D. Hosgood, *JAMA Oncol.* **2018**, 4, 1221; c) S. V. Rajkumar, M. A. Dimopoulos, A. Palumbo, J. Blade, G. Merlini, M.-V. Mateos, S. Kumar, J. Hillengass, E. Kastritis, P. Richardson, *Lancet Oncol.* **2014**, 15, 538.
- [7] a) S. V. Rajkumar, *Lancet* **2016**, 387, 1490; b) N. W. C. J. van de Donk, P. G. Richardson, F. Malavasi, *Blood* **2018**, 131, 13; c) L. Sanchez, Y. C. Wang, D. S. Siegel, M. L. Wang, *J. Hematol. Oncol.* **2016**, 9, 51; d) S. K. Kumar, K. C. Anderson, *Clin. Cancer Res.* **2016**, 22, 5453.
- [8] a) H. M. Lokhorst, T. Plesner, J. P. Laubach, H. Nahi, P. Gimsing, M. Hansson, M. C. Minnema, U. Lassen, J. Krejci, A. Palumbo, N. W. C. J. van de Donk, T. Ahmadi, I. Khan, C. M. Uhlar, J. Wang, A. K. Sasser, N. Losic, S. Lisby, L. Basse, N. Brun, P. G. Richardson, *N. Engl. J. Med.* **2015**, 373, 1207; b) S. Lonial, B. M. Weiss, S. Z. Usmani, S. Singhal, A. Chari, N. J. Bahlis, A. Belch, A. Krishnan, R. A. Vescio, M. V. Mateos, A. Mazumder, R. Z. Orlowski, H. J. Sutherland, J. Blade, E. C. Scott, A. Oriol, J. Berdeja, M. Gharibo, D. A. Stevens, R. LeBlanc, M. Sebag, N. Callander, A. Jakubowiak, D. White, J. de la Rubia, P. G. Richardson, S. Lisby, H. B. Feng, C. M. Uhlar, I. Khan, T. Ahmadi, P. M. Voorhees, *Lancet* **2016**, 387, 1551.
- [9] a) T. Facon, S. Kumar, T. Plesner, R. Z. Orlowski, P. Moreau, N. Bahlis, S. Basu, H. Nahi, C. Hulin, H. Quach, H. Goldschmidt, M. O'Dwyer, A. Perrot, C. P. Venner, K. Weisel, J. R. Mace, N. Raj, M. Attal, M. Tiab, M. Macro, L. Frenzel, X. Leleu, T. Ahmadi, C. Chiu, J. Wang, R. Van Rappelbergh, C. M. Uhlar, R. Kobos, M. Qi, S. Z. Usmani, M. T. Investigators, *N. Engl. J. Med.* **2019**, 380, 2104; b) M. Dimopoulos, H. Quach, M. V. Mateos, O. Landgren, X. Leleu, D. Siegel, K. Weisel, H. Yang, Z. Klippel, A. Zahlten-Kumeli, S. Z. Usmani, *Lancet* **2020**, 396, 186; c) M. V. Mateos, M. A. Dimopoulos, M. Cavo, K. Suzuki, A. Jakubowiak, S. Knop, C. Doyen, P. Lucio, Z. Nagy, P. Kaplan, L. Pour, M. Cook, S. Grosicki, A. Crepaldi, A. M. Liberati, P. Campbell, T. Shekhova, S. S. Yoon, G. Iosava, T. Fujisaki, M. Garg, C. Chiu, J. Wang, R. Carson, W. Crist, W. Deraedt, H. Nguyen, M. Qi, J. San-Miguel, A. T. Investigators, *N. Engl. J. Med.* **2018**, 378, 518.
- [10] A. K. Nooka, J. L. Kaufman, C. C. Hofmeister, N. S. Joseph, T. L. Heffner, V. A. Gupta, H. C. Sullivan, A. S. Neish, M. V. Dhodapkar, S. Lonial, *Cancer* **2019**, 125, 2364.
- [11] a) F. Malard, M. Mohty, *Lancet* **2020**, 395, 1146; b) M. Hussein, *Clin. Lymphoma* **2003**, 4, 18.
- [12] C. Zhou, Y. Xia, Y. Wei, L. Cheng, J. Wei, B. Guo, F. Meng, S. Cao, J. C. M. van Hest, Z. Zhong, *Acta Biomater.* **2020**, 113, 512.
- [13] a) P. Zhang, G. Ling, J. Sun, T. Zhang, Y. Yuan, Y. Sun, Z. Wang, Z. He, *Biomaterials* **2011**, 32, 5524; b) Y. Wang, L. Dou, H. He, Y. Zhang, Q. Shen, *Mol. Pharmaceutics* **2014**, 11, 885; c) C. Wang, M. Zhao, Y.-R. Liu, X. Luan, Y.-Y. Guan, Q. Lu, D.-H. Yu, F. Bai, H.-Z. Chen, C. Fang, *Biomaterials* **2014**, 35, 1215; d) J. A. Silverman, S. R. Deitcher, *Cancer Chemother. Pharmacol.* **2013**, 71, 555.
- [14] a) W. Yang, Y. Zou, F. Meng, J. Zhang, R. Cheng, C. Deng, Z. Zhong, *Adv. Mater.* **2016**, 28, 8234; b) Y. Zou, M. Zheng, W. Yang, F. Meng, K. Miyata, H. J. Kim, K. Kataoka, Z. Zhong, *Adv. Mater.* **2017**, 29, 1703285; c) Y. Jiang, W. Yang, J. Zhang, F. Meng, Z. Zhong, *Adv. Mater.* **2018**, 30, 1800316.
- [15] a) J. H. Peng, J. Chen, F. Xie, W. Bao, H. Y. Xu, H. X. Wang, Y. H. Xu, Z. X. Du, *Biomaterials* **2019**, 222, 13; b) S. Zalba, A. M. Contreras, A. Haeri, T. L. M. ten Hagen, I. Navarro, G. Koning, M. J. Garrido, *J. Controlled Release* **2015**, 210, 26; c) S. A. Shein, I. I. Kuznetsov, T. O. Abakumova, P. S. Chelushkin, P. A. Melnikov, A. A. Korchagina, D. A. Bychkov, I. F. Seregina, M. A. Bolshov, A. V. Kabanov, V. P. Chekhonin, N. V. Nukolova, *Mol. Pharmaceutics* **2016**, 13, 3712.
- [16] a) M. D'Agostino, R. Mina, F. Gay, *Lancet Haematol.* **2020**, 7, e355; b) L. Moreno, C. Perez, A. Zabaleta, I. Manrique, D. Alignani, D. Ajona, L. Blanco, M. Lasa, P. Maiso, I. Rodriguez, S. Garate, T. Jelinek, V. Segura, C. Moreno, J. Merino, P. Rodriguez-Otero, C. Panizo, F. Prosper, J. F. San-Miguel, B. Paiva, *Clin. Cancer Res.* **2019**, 25, 3176; c) I. S. Nijhof, T. Casneuf, J. van Velzen, B. van Kessel, A. E. Axel, K. Syed, R. W. J. Groen, M. van Duin, P. Sonneveld, M. C. Minnema, S. Zweegman, C. Chiu, A. C. Bloem, T. Mutis, H. M. Lokhorst, A. K. Sasser, N. van de Donk, *Blood* **2016**, 128, 959.
- [17] a) W. Gu, J. An, H. Meng, N. Yu, Y. Zhong, F. Meng, Y. Xu, J. J. Cornelissen, Z. Zhong, *Adv. Mater.* **2019**, 31, 1904742; b) Y. Zhong, F. Meng, W. Zhang, B. Li, J. C. van Hest, Z. Zhong, *J. Controlled Release* **2020**, 320, 421.
- [18] Z. Gu, X. Wang, R. Cheng, L. Cheng, Z. Zhong, *Acta Biomater.* **2018**, 80, 288.
- [19] a) D. Douer, *Oncologist* **2016**, 21, 840; b) C. E. M. Gidding, S. J. Kellie, W. A. Kamps, S. S. N. de Graaf, *Crit. Rev. Oncol. Hematol.* **1999**, 29, 267.
- [20] a) E. Terpos, I. Ntanasis-Stathopoulos, M. Gavriatopoulou, M. A. Dimopoulos, *Blood Cancer J.* **2018**, 8, 12; b) S. Rasch, T. Lund, J. T. Asmussen, A. Lerberg Nielsen, R. Faabo Larsen, M. Osterheden Andersen, N. Abildgaard, *Cancers* **2020**, 12, 2113.
- [21] a) Q. Hu, C. Qian, W. Sun, J. Wang, Z. Chen, H. N. Bomba, H. Xin, Q. Shen, Z. Gu, *Adv. Mater.* **2016**, 28, 9573; b) A. Swami, M. R. Reagan, P. Basto, Y. Mishima, N. Kamaly, S. Glavey, S. Zhang, M. Moschetta, D. Seevaratnam, Y. Zhang, J. Liu, M. Memarzadeh, J. Wu, S. Manier, J. Shi, N. Bertrand, Z. N. Lu, K. Nagano, R. Baron, A. Sacco, A. M. Roccaro, O. C. Farokhzad, I. M. Ghobrial, *Proc. Natl. Acad. Sci. U. S. A.* **2014**, 111, 10287.
- [22] a) J. D. Ashley, J. F. Stefanick, V. A. Schroeder, M. A. Suckow, N. J. Alves, R. Suzuki, S. Kikuchi, T. Hideshima, K. C. Anderson, T. Kiziltepe, *J. Controlled Release* **2014**, 196, 113; b) N. Kotagiri, M. L. Cooper, M. Rettig, C. Egbulefu, J. Prior, G. Cui, P. Karmakar, M. Zhou, X. Yang, G. Sudlow, *Nat. Commun.* **2018**, 9, 275.
- [23] a) P. de la Puente, M. J. Luderer, C. Federico, A. Jin, R. C. Gilson, C. Egbulefu, K. Alhallak, S. Shah, B. Muz, J. Sun, *J. Controlled Release* **2018**, 270, 158; b) Y.-H. Huang, M. R. Vakili, O. Molavi, Y. Morrissey, C. Wu, I. Paiva, A. H. Soleimani, F. Sanaee, A. Lavasanifar, R. Lai, *Cancers* **2019**, 11, 248.
- [24] a) S. Kumar, B. Paiva, K. C. Anderson, B. Durie, O. Landgren, P. Moreau, N. Munshi, S. Lonial, J. Bladé, M.-V. Mateos, M. Dimopoulos, E. Kastritis, M. Boccadoro, R. Orlowski,

- H. Goldschmidt, A. Spencer, J. Hou, W. J. Chng, S. Z. Usmani, E. Zamagni, K. Shimizu, S. Jagannath, H. E. Johnsen, E. Terpos, A. Reiman, R. A. Kyle, P. Sonneveld, P. G. Richardson, P. McCarthy, H. Ludwig, W. Chen, M. Cavo, J.-L. Harousseau, S. Lentzsch, J. Hillengass, A. Palumbo, A. Orfao, S. V. Rajkumar, J. S. Miguel, H. Avet-Loiseau, *Lancet Oncol.* **2016**, *17*, e328; b) S. V. Rajkumar, *Am. J. Hematol.* **2020**, *95*, 548; c) A. Romano, G. A. Palumbo, N. L. Parrinello, C. Conticello, M. Martello, C. Terragna, *Front. Oncol.* **2019**, *9*, 699.
- [25] a) N. Raje, G. D. Roodman, *Clin. Cancer Res.* **2011**, *17*, 1278; b) A. Mansour, A. Wakkach, C. Blin-Wakkach, *Front. Immunol.* **2017**, *8*, 10; c) S. Marino, G. D. Roodman, *Cold Spring Harb. Perspect. Med.* **2018**, *8*, 21.
- [26] a) K. Chen, P. C. Qiu, Y. Yuan, L. Zheng, J. B. He, C. Wang, Q. Guo, J. Kenny, Q. Liu, J. M. Zhao, J. H. Chen, J. Tickner, S. W. Fan, X. F. Lin, J. K. Xu, *Theranostics* **2019**, *9*, 1634; b) I. Veletic, T. Manshouri, A. S. Multani, C. C. Yin, L. Chen, S. Verstovsek, Z. Estrov, *Blood* **2019**, *133*, 2320.
- [27] a) A. Bouchnita, N. Eymard, T. K. Moyo, M. J. Koury, V. Volpert, *Am. J. Hematol.* **2016**, *91*, 371; b) R. Lancet Oncol Khan, S. Apewokin, M. Graziutti, S. Yaccoby, J. Epstein, F. van Rhee, A. Rosenthal, S. Waheed, S. Usmani, S. Atrash, S. Kumar, A. Hoering, J. Crowley, J. D. Shaughnessy, B. Barlogie, *Leukemia* **2015**, *29*, 1195; c) C. Sirac, G. A. Herrera, P. W. Sanders, V. Batuman, S. Bender, M. V. Ayala, V. Javaugue, J. Teng, E. A. Turbat-Herrera, M. Cogné, *Nat. Rev. Nephrol.* **2018**, *14*, 246.